ACMI: FM-Based Indoor Localization via Autonomous Fingerprinting

Sungro Yoon, Kyunghan Lee, *Member, IEEE*, YeoCheon Yun, and Injong Rhee, *Member, IEEE*

Abstract—We present ACMI, an FM-based indoor localization system that does not require proactive site profiling. ACMI constructs the fingerprint database based on pure estimation of indoor received signal strength (RSS) distribution, where only the signals transmitted from commercial FM radio stations are used. Based on extensive field measurement study, we established our own signal propagation model that harnesses FM radio characteristics and open information of FM transmission towers in combination with the floor-plan of a building. Output of the model is an RSS fingerprint database. Using the fingerprint database as a knowledge base, ACMI refines a positioning result via the two-step process; parameter calibration and path matching, during its runtime. Without site profiling, our evaluation indicates that ACMI in seven campus locations and three downtown buildings using eight distinguished FM stations finds positions with only about 6 and 10 meters of errors on average, respectively.

Index Terms—Indoor localization, FM signal, signal fingerprint, pattern matching

1 Introduction

The prevalence of smart devices has triggered the recent emergence of location-based services. While *anywhere* services is expected, however, satellite signals do not reach inside the buildings and therefore the global positioning system (GPS) is not available indoors. To address this issue, there has been an urgent call for an accurate indoor localization technique.

Received signal strength (RSS) based techniques have been actively discussed among several branches of studies. They are known to provide robust and accurate indoor localization [1], [2]. The RSSs from various signal sources form a position-specific signature. Thus given the signature DB, a mobile user can query the current location based on the sampled RSSs. The merit is that this technique achieves good accuracy without the need for an installation of any new infrastructure nor any complicated hardware and software. But the difficulty is with an exhaustive preprocess of site profiling, where every single spot in a building should be probed to store the corresponding RSS samples. This process is labor-intensive and time-consuming, thus becoming the major bottleneck that hinders the technique from being widely deployed in the real world.

Crowdsourcing is an alternative way to the manual site profiling. Crowdsourcing distributes the heavy load by asking each mobile user to contribute to build the fingerprint database collaboratively. But in this approach it is hard to expect that a mobile user can label the sampled RSSs with precise location, because the current location is not known to the user a priori at the moment. Therefore inputs with at most room-level accuracy might be expected [3], [4]. Recent innovations [5], [6], [7] solve this problem with dead-reckoning powered by motion sensors (e.g., accelerometer, compass, etc.) and the knowledge of floorplans or landmarks. Therefore the mobile users, unawarely, can report the current location with measured RSS samples. Although this alleviates the issue, still, some non-negligible time duration might be required to stabilize the database and to start the localization service.

Another challenge with the current RSS fingerprint based localization is the vulnerability of the signal source itself. WiFi is being commonly used for the RSS-based techniques because of its abundance in the availability. It has been reported however that the WiFi signals, around 2.4 GHz or 5 GHz, are very susceptible to human presence or orientation of mobile devices [8]. Moreover the WiFi APs are deployed without careful planning in many cases and therefore their configuration might be easily changed by individuals. This means that even with the extensive site profiling efforts, after some time, it is highly probable that the RSSs sampled by mobile users do not match accurately with pre-surveyed RSSs.

In this paper, we present ACMI, a system named after Autonomous signal DB Construction and Matching of Indoor RSS fingerprint database. We choose FM broadcasts as the signal source. Enabled by the excellent stability of this medium [9] we build the fingerprint database purely based on the indoor signal propagation model. Thus the site profiling efforts can be saved. Consider a scenario where an IT technician sends necessary information to a third party service provider. Based on the model and the given information, the service provider can immediately generate and offer the RSS fingerprint database.

There have been such model-based approaches [10], [11], [12] in the literature. These proposals use WiFi signal to achieve good accuracy, but we strongly believe that the

- *S. Yoon is with the Microsoft, Bellevue, WA 98005. E-mail: sungro.yoon@microsoft.com.*
- *K. Lee and Y. Yun are with the School of Electrical and Computer Engineering, UNIST, Korea. E-mail: {khlee, ycyun}@unist.ac.kr.*
- *I. Rhee is with the Department of Computer Science, North Carolina State University, Raleigh, NC 27695. E-mail: rhee@ncsu.edu.*

Manuscript received 10 Nov. 2013; revised 28 Mar. 2015; accepted 20 July 2015. Date of publication 6 Aug. 2015; date of current version 3 May 2016. For information on obtaining reprints of this article, please send e-mail to: reprints@ieee.org, and reference the Digital Object Identifier below. Digital Object Identifier no. 10.1109/TMC.2015.2465372

model-based technique can better be realized with FM signals. The major benefit is that FM signals are stable and have a city-wide coverage. Also the essential information for the model, such as global coordinate of transmission antenna, transmission power, etc., is readily available [13]. Unless manually surveyed, such information about WiFi APs is not known beforehand. WiFi coverage is small and there are a number of APs heterogeneously deployed with such unknown characteristics even in a single building. Finally, it has been recently shown that FM-based localization can provide very good accuracy. Chen et al. showed that FM fingerprint-based indoor localization can achieve 92 percent room identification and up to 1 ft. localization accuracy [9].

The challenge we face is that, to the best of our knowledge, there does not exist a model that estimates the indoor RSS distribution of FM signals, transmitted from remote stations usually tens of miles away. Through extensive in-building measurements we have found that a few dominating rules exist, which determine the RSS at a certain indoor spot. We develop an empirical model conforming to the rules. The evaluation shows the impressive similarity between the model-based estimation and the actual measurements. Using this model and signals from 8 FM stations, simple minimum squared error (MSE) match shows the accuracy between 10 m and 18 m without any calibration. We further demonstrate that the accuracy can be improved with online operations. We perform least mean square (LMS) based runtime parameter calibration, and then perform path matching based positioning. Extensive evaluation performed in seven different sites over 1,100 spots shows that our system can achieve average 89 percent room identification and 6 m localization accuracy.

We outline our contributions as follow. (1) We propose a novel FM-model based indoor localization that can avoid the site profiling. (2) For this we perform extensive indoor measurements and suggest a practical model that predicts the RSS distribution only using the publicly available FM transmission information and the floorplan of a building. (3) We propose an online calibration and inference technique that can improve the localization accuracy. (4) Finally we perform extensive evaluation and show that the system achieves good accuracy in real-world scenarios.

The rest of this paper is organized as follows. In Section 2, we discuss relevant studies. Then we describe our findings from indoor measurements in Section 3 and establish an empirical model in Section 4. The system is described in Section 5 and we further discuss several issues in Section 6. The performance is evaluated in Section 7 and finally Section 8 concludes the paper.

2 Related Work

2.1 Fingerprint-Based Techniques

RADAR [1] has pioneered the RSS fingerprint-based indoor localization. At each indoor location, broadcast packets from WiFi APs are overheard. The RSSs from multiple APs form a single vector representing the specific location and by performing look-ups within the pre-built database the current location can be found. Horus [2] advances the technique by introducing a probability based inference model, where the RSS from an AP is modeled into a random variable that varies according to time and location. Apart from the RSS, a recent technique [14] utilizes the channel impulse response of WiFi as the location-specific signature and achieves highly accurate indoor localization. While these techniques are very accurate, they require the labor and time intensive site profiling where every indoor spot should be manually matched with corresponding fingerprints. In case WiFi is used as the signal source, this site profiling should be performed repetitively due to the significant temporal variances of WiFi signals.

Crowdsourcing is an alternative way for sharing the load among multiple users. The problem is that it is difficult for such mobile users to label the collected RSS samples with accurate location information [3], [4]. Recent innovations [5], [7] solve this problem by the use of the floorplan and the movement detector. Still, it takes time for convergence of the fingerprint DB.

2.2 Model-Based Techniques

To avoid the manual profiling processes researchers suggested to automatically generate the look-up DB, based on known radio wave propagation characteristics [10], [11], [12]. Lim et al. proposed a technique [12] that, by observing WiFi RSSs and finding the linear relationship with geographic distances, builds the signal-distance map. This signal-distance map can be used to locate a mobile user's location. Ez [10] also builds RSS-distance equations, but exploits genetic algorithm to solve the equations. These two techniques basically base upon log-distance propagation model but do not explicitly assume any prior knowledge about infrastructures or deployments. They automatically obtain essential information from a few initial measurements. ARIADNE [11] uses floorplan together with sophisticated ray tracing method. By using known locations of WiFi APs and transmission powers, it can automatically generate the look-up DB.

Modeling approaches other than RSS also exist such as time of arrival [15], time difference of arrival [16] and angle of arrival [17]. They achieve highly accurate localization. However, these techniques require complicated processing in either software or hardware.

2.3 FM-Based Localization

There have been growing research interests regarding FM-based *outdoor* localization. The advantage is that FM signals cover very wide area (up to 300 km) and are globally available, and FM radios consume less power compared to GPS or WiFi, mainly due to much smaller bandwidth. FM signal can be used to detect a mobile user [18] or a passing object [19], [20], [21] outdoors. However, these techniques do not provide sufficient accuracy for the indoor localization. Being mostly based on time of arrival differentiation, a few tens of meters might be achieved only when line of sight (LoS) exists between senders and receivers. Youssef et al. showed the feasibility of the FM-modeling-based technique in an outdoor setup [22]. Based on the signal strength model and the calibration, 8 km accuracy has been achieved. But the main difficulty with the RSS-based approach is that the RSSs of FM signals do not significantly vary within nearby outdoor locations because of the strong transmission

TABLE 1
Summary of Localization Techniques

Technique	Accuracy	Labor cost	Info. cost
Fingerprint-based	<1 m	High	Low
Crowdsourcing	<5 m	High (distributed)	Low
Model-based	<5 m	Low	High
Dead-reckoning	$\gg$10 m	Low	Low
ACMI	$\approx$5 m	Low	Low

power (i.e., near-field effect). Therefore, close-by areas within small distances are often indistinguishable with FM RSSs. The linear relationship between the displacement and the signal phase of FM pilot tone can be considered [23] but it has not been verified experimentally.

Recent studies showed the feasibility of FM-based indoor localization as well [9], [24]. Unlike the outdoor environment, indoor structures create various shadow-like attenuation patterns that can be preferably used as signatures for the positioning. Chen et al. showed that up to 92 percent room level identification can be achieved with FM RSS pattern alone [9]. In the meanwhile, they showed that the FM signals are robust to fading, human presences and changes in mobile devices' orientations unlike WiFi. Also FM signals do not experience temporal variations as much as WiFi signals.

Table 1 summarizes the techniques introduced so far. Fingerprint-based techniques outperform others in terms of accuracy. But this is at the prohibitive cost of site profiling. While crowdsourcing can offload the profiling efforts, it needs to reorganize the crowd-sourced information and filter out ambiguities. Signal modeling is the key to eliminating the site profiling efforts. But most existing model-based approaches rely on WiFi as signal sources. It is non-trivial to collect the WiFi signal characteristics accurately. Moreover, the information should be refreshed periodically to keep the model accurate because the collected information can change over time. Dead-reckoning uses motion sensors to observe the user movement. Despite its versatility, the accuracy quickly drops over time due to the sensing errors. So other techniques are usually accompanied to compensate for the errors. ACMI does not require any site profiling but still achieves reasonably good accuracy by effectively utilizing public information which is always up to date. ACMI uses an FM receiver and motion sensors, which are commonly equipped or at least can be equipped at a low cost in the state-of-the-art smartphones.

2.4 Indoor Propagation Models

The well-known log-distance propagation model estimates the signal strengths of radio signals as

$$P(d) = P(d_0) - 10 \cdot n \cdot log_{10}\left(\frac{d}{d_0}\right) \ [dBm],$$

where $P(d)$, the received power at distance d is given by subtracting the attenuation factor from $P(d_0)$, the signal strength at reference distance d_0, usually set to 1m. Here n is the path loss exponent that is obtained experimentally. This simple log-distance model is not accurate indoors for following reasons. First, there could be obstacles between the transmitter and the receiver that further attenuate the signals. Second, this model assumes that the transmission power is equal (isotropic) in all directions, while nowadays many WiFi APs occupy antenna arrays or directional antennas and therefore they are non-isotropic. Finally, this model does not take into consideration the non-line-of-sight indirect signals that traverse longer paths than the direct signals.

To overcome the inaccuracy of log-distance model with indoor signal propagation, empirical models have been proposed [25], [26], [27]. While these models accurately estimate the indoor signal strengths, most of them considered only high signal frequencies ($\geq$900 MHz) that are commonly used for the wireless communication. These frequency bands have significantly different characteristics compared to FM signals at very high frequency (VHF) that range from 30 to 300 MHz; the propagation of higher frequency signals is very rectilinear, while VHF signals around 100 MHz experience severe diffraction. Also, those studies only consider the case where a transmitter is inside the building. In our model, we consider the indoor propagation of FM broadcast signal where the transmitters are usually tens of miles away.

Another line of study [28], [29], [30] is to build a mathematical model. The ray tracing technique was originally used in 3D graphics analysis. It tracks virtually infinite number of very small *ray tubes* that stem out from the transmitter. Direct propagation, reflection and diffusion of a radio wave can be accurately modeled by the ray tube. Accumulating the ray tubes at each spot on the floor, the ray tracing can accurately predict the indoor RSS distribution. But the ray tracing cannot be used in our system for the following two reasons. First, the transmitter is too far away, which makes it impossible to model the traversal path of ray tubes. It is not known which obstacles are in between the building and FM transmitters. Second, the ray tracing technique is computationally complex. Computation of a scenario where the transmitter is just tens of meters away takes several hours [30]. Therefore, in our case the heavy computation may kill the practicality of our system. But we can consider this as one of future work.

3 Measurement and Observation

In this section, we describe our findings from experimentations. The findings will be used to design the empirical indoor propagation model in the next section. Note that we do not make any assumption or adjustment to existing *outdoor* path loss models. We adopt one of outdoor path loss models [31] to estimate the RSSs at outer walls of a building and use the values as the basis of our indoor propagation model.

3.1 Measurement Methodology

We separately perform measurements outside and inside the building. We use USRP1 assembled with basic-RX daughterboard and FM Terk Pro antenna. RSSs of broadcast signals from eight FM stations are measured in a round-robin way at each position. The locations of those FM stations are shown in Fig. 1 and other information is listed in Table 2. While there are a few more stations in the vicinity, we only select these stations based on the availability of signals in buildings.

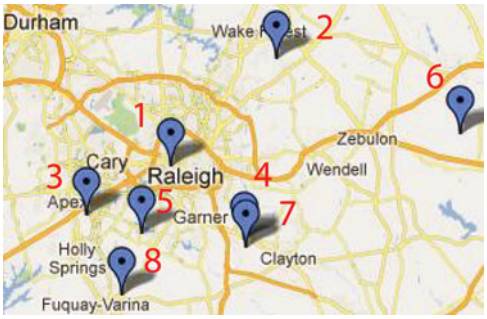

Fig. 1. Locations of eight available FM stations in the vicinity.

TABLE 2
Information of FM Stations that We Used for Our Measurements

ID	Freq. (MHz)	P_{Tx}(kW)	Height(m)	Dist.(km)
1	88.1	25	79	2.1
2	89.7	100	359	29.3
3	93.9	100	453	16.6
4	94.7	95	511	18.9
5	96.1	98	300	10.4
6	100.7	4.3	489	59.6
7	101.5	96	555	19.8
8	105.1	73	339	21.0

Please note that we use the high performance antenna to observe the RSSs with finer granularity. But this is not required in the real application. We discuss the impact of the antennas in Section 7.3.

For the measurement study we need transmission information of FM radio. This includes coordinates of FM towers, transmission power, antenna direction and height. Such information is managed by Federal Communications Commission (FCC). FCC provides a query database which is accessible via web interface [13]. We also use the building information including the coordinates of a building and the floorplan. Each item is elaborated in the following.

Coordinate of FM tower. The coordinates of an FM tower is provided as Fig. 2a shows. The global longitude and latitude information is required to calculate (1) distance and (2) direction toward the local building. The distance is used to estimate the outdoor path loss. The direction is required to calculate the net transmission power and also to analyze the indoor RSS distribution (e.g., to figure out LoS and NLoS windows).

Transmission power and antenna direction. As an FM transmission tower is usually installed outside a city, the antenna is commonly directed towards the inner city for the power efficiency. So both the transmission power and antenna direction is required together to obtain the net transmission power. The transmission power is shown in Fig. 2a. FCC provides antenna direction information in the form of relative field plot, as Fig. 2b shows.

Antenna height. Antenna height has an impact on the outdoor path loss. Signals from higher antenna experience less obstacles and thus less path loss [31]. The height of a transmission tower is given in Fig. 2a.

Coordinates of local building. This is required to compute the distance and the direction between the transmission tower and the local building. Today's map applications (e.g., Bing Map) provides high-resolution coordinates of buildings in most of major cities.

Floor plan. Floor plan has the internal structure information of a building and therefore is essential for the estimation of RSS distribution over the floor. Our model needs the topology information of exterior walls, interior walls, and windows. We import the structural information in our software and process such that each object (e.g., wall and window) is assigned its own global coordinate. Finally, the transmission towers and the indoor structures are organized in a single data structure representing the global topology, shown in Fig. 8.

3.2 Outside the Building

The purpose of this measurement is to test the accuracy of outdoor RSS estimation. In other words, we would like to see if we can accurately estimate the RSSs at the surface of a building given only the public information. These outdoor RSSs will naturally define the maximum of indoor RSS values. We measure the RSS of FM signals at the roof top of a building and compare with estimated values.

The RSS outside the building is estimated to be

$$RSS = Net\ Tx\ Power - Path\ Loss\ [dBm],$$

where the net transmission power indicates the actual transmitted power from the transmission antenna to the direction towards the local building. Usually an FM transmission antenna is *directional* and so the field strength of an FM transmission antenna differs at each direction. The net transmission power is calculated by multiplying *normalized relative field strength* to the original transmission power (See Fig. 11b). Thus it is required to calculate the actual direction from the transmission tower to the local building using the global coordinates (longitude and latitude).

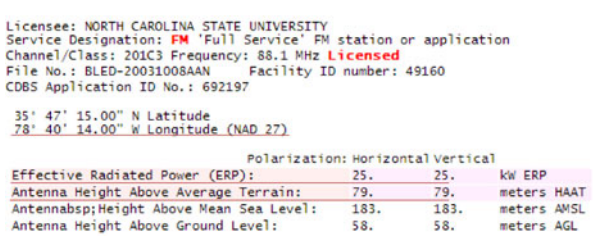
Licensee: NORTH CAROLINA STATE UNIVERSITY
Service Designation: FM 'Full Service' FM station or application
Channel/Class: 201C3 Frequency: 88.1 MHz Licensed
File No.: BLED-20031008AAN Facility ID number: 49160
CDBS Application ID No.: 692197

35° 47' 15.00" N Latitude
78° 40' 14.00" W Longitude (NAD 27)

Polarization:	Horizontal	Vertical	
Effective Radiated Power (ERP):	25.	25.	kW ERP
Antenna Height Above Average Terrain:	79.	79.	meters HAAT
Antennabsp;Height Above Mean Sea Level:	183.	183.	meters AMSL
Antenna Height Above Ground Level:	58.	58.	meters AGL

(a) Coordinate & height of Tx tower.

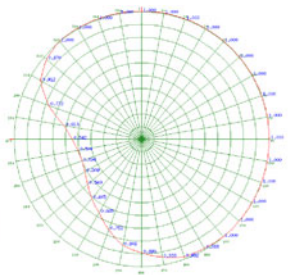

(b) Relative field polar plot of transmission antenna.

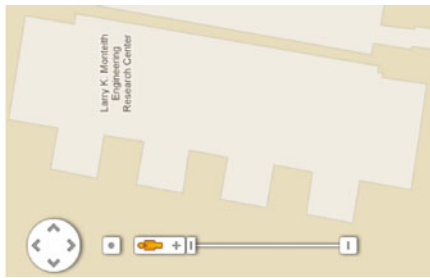

(c) Coordinate of building.

Fig. 2. Required information for building the fingerprint DB.

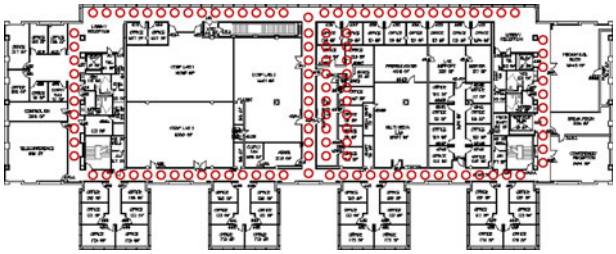

Fig. 3. Floorplan of building. Red dots represent the spots where RSSs have been sampled.

We refer a technique from previous studies [31], which takes transmission power, antenna height and distance between a transmitter and a receiver. The RSSs outside the building are estimated based on this path loss model and compared with the actual measurements in Fig. 4. The average estimation error is 3.8 dB for all FM stations. Note that the estimation error for the station 1 is significantly larger than those of other stations. We analyze that the reason should be the lower height of the transmission tower. The height of the this transmission tower is 79 m while other towers are 430 m in average. Therefore the signals might be frequently blocked by obstacles during the traversal path. With the similar reason, we find that signals from remote stations tend to experience larger path loss compared to adjacent stations (e.g., station 2, 6 and 8).

3.3 Inside the Building

We perform indoor measurements to observe how internal structures of a building create various RSS patterns. We measure RSSs in 375 spots within a 35 m by 95 m office building shown in Fig. 3. Each spot is around 2 feet away from each other. Below, we list the findings that we observed from the measurement data.

3.3.1 *"Windows Are the Main Entrances of FM Signals into a Building"*

VHF signals cannot usually penetrate through the surface of a building. They experience huge attenuation when blocked by the exterior walls. On the other hand, the signals can pass through windows and enter into the building with relatively small attenuation. Interestingly, we found that the amount of attenuation depends upon the direction that the window is facing.

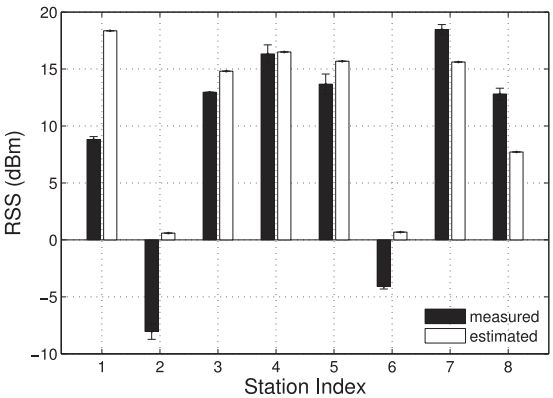

Fig. 4. The measured and estimated RSSs outside the building. Average error is 3.8 dB.

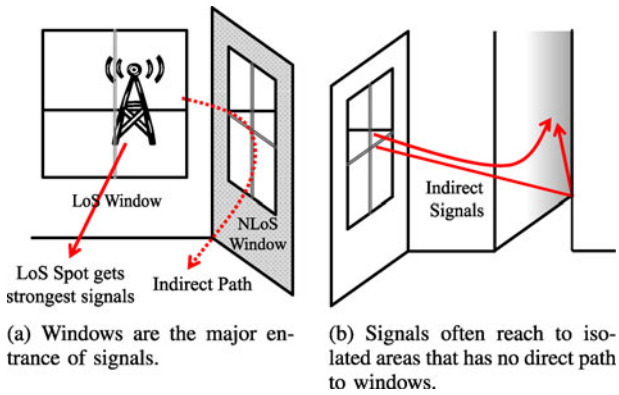

Fig. 5. Indoor propagation characteristics of FM broadcast signals.

Line of sight window. If an FM transmission tower is in the direction that a window is facing, at a certain indoor spot, we call each as the *LoS window* and the *LoS spot* as shown in Fig. 5a. LoS windows are the main source of FM signals in the building and the LoS spot located right beside the LoS window gets the strongest RSS of that FM broadcast. While there could be many windows in a building, the RSSs near the LoS windows are almost same with only negligible variances. Fig. 6 compares RSSs at building surface, LoS windows, NLoS windows and the average RSSs. We see that an LoS spot beside LoS windows gets the strong RSSs, almost comparable to the RSS outside the building.

Non-LoS window. Even though an indoor spot does not have an LoS path to the transmission tower, if that spot has a rectilinear path to *any other window* the spot also gets relatively strong signals. The reason is that VHF signals, after being blocked by exterior walls, can still enter the *Non-LoS windows* from other sides via indirect paths. The indirect paths are shown as a dotted line in Fig. 5a. Unlike the LoS window case, Fig. 6 shows that the RSSs at the NLoS windows are not regular. This is mainly because the traversal paths of NLoS signals are affected by the outer structures of a building. But we observe that the RSSs at NLoS windows are still stronger than average indoor RSSs.

Size of window. A radio wave can freely pass through a hole only when diameter of the hole is larger than its wavelength. Recall a microwave oven; while one can see inside the oven via visible rays, the microwave radiation still cannot pass through the metal mesh since the diameter of the mesh is smaller than the wavelength. From our observation,

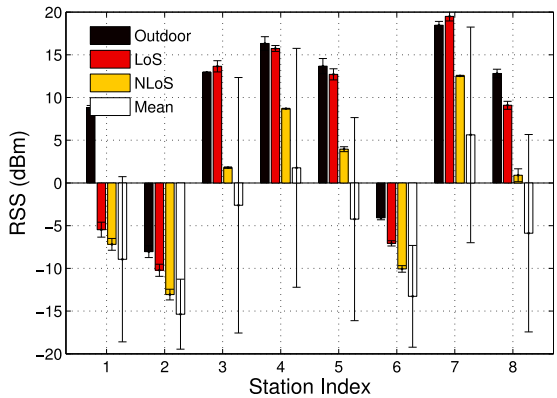

Fig. 6. The RSSs at outside the building, windows with LoS, without LoS and average values are compared and averaged at 60 different spots.

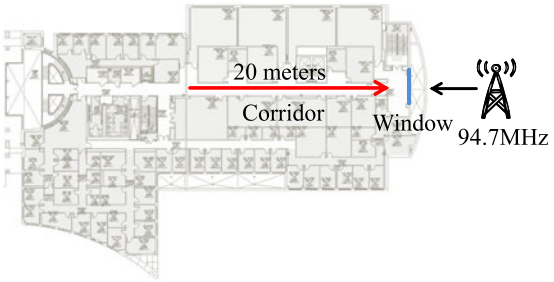

(a) Path loss measurement methodology.

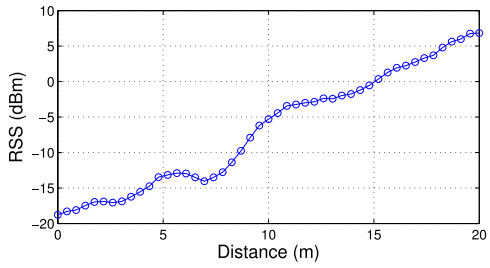

(b) Indoor path loss measurement results.

Fig. 7. Pass loss measurement at an indoor corridor shows the path loss exponent of 2.16.

the FM signals are significantly attenuated when the size of a window is less than half the wavelength, which is around 1.5 meters with 100 MHz signals.

3.3.2 "Indoor Walls Significantly Attenuate the Signals"

Indoor walls block the direct propagation of signals and significantly attenuate the RSS. Empirical studies [26], [27] report that the amount of attenuation increases linearly proportional (in log-scale) to the number of obstacles during the path. We also observe the similar trends. We performed measurements to see the RSS attenuation when signals propagate across walls. In order to accurately measure the attenuation caused only by walls, we chose 30 LoS spots and 30 nearby spots right behind the walls. The actual distance between each pair is less than 2 m. Then we measured the RSS at those spots. For signals from eight stations, the attenuation was 6.9 dB in average. But this depends on the material of the wall and can vary across buildings.

3.3.3 "Signals Experience Significant Indoor Path Loss"

Indoor attenuation of FM signals is much larger than outside. We measure the amount of path loss, while varying the distance to the LoS window. To accurately measure the impact of path loss we choose a different building for this measurement only. The building has a corridor with a large window at one end as shown in Fig. 7a. We measure the RSSs of LoS signals while moving 20 meters. The result is shown in Fig. 7b and the average path loss exponent is 2.16. But as previous studies show [26], [27], the path loss exponent widely varies with environments.

3.3.4 "Signals Frequently Take Indirect Paths to Reach Isolated Areas"

An isolated spot, which does not have a direct path to any window, still gets signals. The reason is that VHF signals can detour when facing obstacles and often reach to isolated areas, as illustrated in Fig. 5b. Such signals would include diffraction, diffusion and reflection. But we just refer them as indirect signals since they arrive simultaneously and thus are not differentiable.

Large portion of VHF signals takes indirect paths. So the isolated spots often exhibit higher RSSs at VHF than they should at higher carrier frequencies. We refer an indoor spot, which has a direct path to any window and no obstacle in-between, as *direct spot*. The direct spot includes both the LoS and the NLoS spots. We find that the isolated spots exhibiting higher RSSs usually have clear paths to those direct spots. As a result, the RSSs at those isolated spots never exceed those of the nearest direct spots and decrease with the distance to those direct spots. We perform the similar experiment as above to see the path loss of the indirect signals and the result was similar. So we omit the result here.

4 Model and Verification

We suggest an empirical model based on our observation. The model is given as follows:

$$RSS(s,t) = \max[RSS_{LoS}(s,t), RSS_{NLoS}(s,t), RSS_{ind}(s,t)], \quad (1)$$

where $RSS(s,t)$ is the estimated RSS of signals from FM station t, at an indoor spot s and the rests are RSSs received via three different paths. While each RSS via the different path should be summed up in reality, we rather choose to take the maximum out of three for the following reasons. First, we want to keep the linearity of RSS equation in logarithm scale, which is preferable for the online calibration. The summation process will require the conversion of each RSS component into linear scale and therefore include exponential terms such as $RSS = 10 \cdot log_{10}(10^{RSS_{LoS}/10} + 10^{RSS_{NLoS}/10} + 10^{RSS_{ind}/10})$. Those exponential terms hinder the use of linear algorithm that we will adapt for the calibration. Second, there is no great difference between maximum and summation, in dB scale, since one of the RSS components is usually significantly larger than others.

RSS_{LoS} is the portion received via the LoS path:

$$RSS_{LoS}(s,t) = max(RSS(t)) - \alpha \cdot 10 \cdot log_{10}(d/d_0) - n \cdot f, \quad (2)$$

where $max(RSS(t))$ is the maximum indoor RSS of signals from station t. The term is derived from the outdoor path loss model described in Section 3.2. α is the path loss exponent, d is the distance from s to the source of signal (e.g., LoS window in this case), d_0 is the reference distance (1 m), n is the number of walls between the spot and the LoS window and f is the wall attenuation factor. In the same manner, RSS_{NLoS} is the RSS via NLoS windows given as

$$RSS_{NLoS}(s,t) = max(RSS(t)) - \alpha \cdot 10 \cdot log_{10}(d/d_0) - n \cdot f - C_1, \quad (3)$$

where C_1 is the constant attenuation factor of LNoS signals. As described in Section 3.3.1, C_1 is hard to model since the amount of attenuation is not regular. For now we bear the modeling error that arises by setting this value into constant and try to alleviate via online techniques.

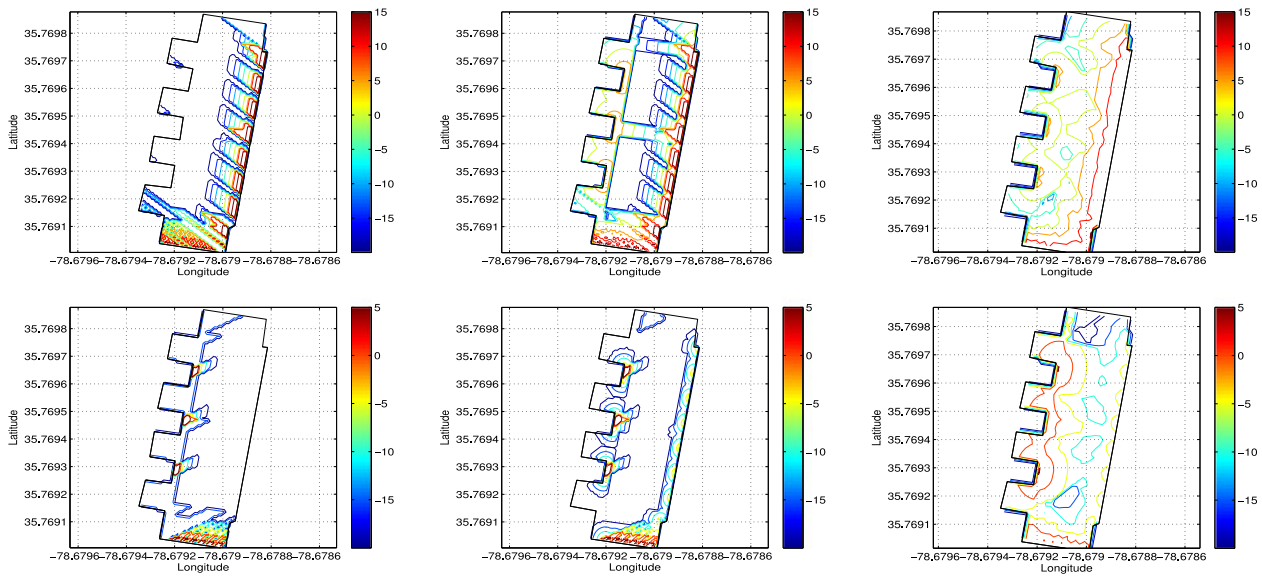

Fig. 8. Model-generated RSS distributions over the floor. Each column demonstrates each algorithm step: (1) LoS signals only, (2) NLoS signals added, and (3) indirect signals added, respectively. Each row is the distribution of signals from station 4 and 8. The FM stations are located south east and south west of the building, respectively. For the floorplan of the building, please see Fig. 3.

In case the size of either an LoS window or an NLoS window is smaller than half the wavelength, around 1.5 m with VHF signals, we subtract the small window attenuation factor, C_2 from the RSS.

Finally, RSS_{ind} is the RSS of signals delivered from other direct spots via an indirect path:

$$RSS_{ind}(s,t) = RSS(u,t) - \alpha \cdot 10 \cdot log_{10}(d/d_0), \qquad (4)$$

where u is the nearest direct spot from s and d is the distance to u. Note that any of RSS_{LoS}, RSS_{NLoS} and RSS_{ind} can be dominant at an indoor spot depending on the indoor structure. For example, RSS_{ind} will be the most significant component at places where there does not exist any window, e.g., the shaded corridor in Fig. 5b.

Algorithm 1, which uses floorplan and FM transmission information as inputs, describes the step by step procedure of obtaining $RSS(s,t)$ from our model. Each column of Fig. 8 shows the change in model output as: RSS_{LoS}, $\max(RSS_{LoS}, RSS_{NLoS})$, and $\max(RSS_{LoS}, RSS_{NLoS}, RSS_{ind})$, respectively. In the figure, the RSS values estimated from FM station 4 and 8 are plotted in each row. As Fig. 8 demonstrates, $RSS(s,t)$ is resulted from a mixture of RSS_{LoS}, RSS_{NLoS} and RSS_{ind}, and is not dominated by one of them.

4.1 Procedures of Estimating Parameters

There are parameters α, f and C_1 required to run our model. We basically use the parameters measured from our experiment. For instance, we use measured indoor path loss exponents 2.16 for α. In this way, we establish the model using 764 data points collected from two different indoor sites in the campus. At each site we used signals from eight different FM stations. Since we observe that the parameters vary at different environments, we take the measured parameters as initial seeds for our online training algorithm and calibrate them during the runtime. The online training algorithm is described in Section 5.3.1. For C_2, we just regard as if there is a wall right in front of the window. Therefore we subtract a constant value f from the expected RSS. So C_2 and f are constantly the same.

Algorithm 1. BuildRSSDatabase(S, T, W, R)

Input: set S, coordinates of all indoor spots
Input: set T, coordinates of all FM stations
Input: set W, coordinates of all windows
Output: RSS(s, t) for $\forall s \in S, \forall t \in T$
for $t \in T$ **do**
  for $s \in S$ **do**
    $RSS_{LoS} \leftarrow 0$, $RSS_{NLoS} \leftarrow 0$;
    if $\exists w \in W$ *such that* w, s *and* t *are on a straight line* **then**
      $d \leftarrow$ distance to the nearest w;
      $n \leftarrow$ number of walls between s and w;
      $RSS_{LoS} \leftarrow max(RSS(t)) - 10\alpha log(d/d_0) - n \cdot f$;
      if *size of* $w < \lambda/2$ **then**
        $RSS_{LoS} = RSS_{LoS} - C_2$;
      end
    end
    if $\exists w \in W$ *such that* $w = NLoS; window$ **then**
      $d \leftarrow$ distance to the nearest w;
      $n \leftarrow$ number of walls between s and w; $RSS_{NLoS} \leftarrow max(RSS(t)) - 10\alpha log(d/d_0) - n \cdot f - C_1$;
      if *size of* $w < \lambda/2$ **then**
        $RSS_{NLoS} = RSS_{NLoS} - C_2$;
      end
    end
    $RSS(s,t) \leftarrow max(RSS_{LoS}, RSS_{NLoS})$;
  end
end
for $t \in T$ **do**
  U: set of spots with direct paths to any $w \in W$;
  for $s \in S$ **do**
    $RSS_{ind} \leftarrow 0$;
    if s *has a direct path to any* $u \in U$ **then**
      $d \leftarrow$ distance to u;
      $RSS_{ind} \leftarrow RSS(u,t) - 10\alpha log(d/d_0)$;
    end
    $RSS(s,t) \leftarrow max(RSS(s,t), RSS_{ind})$;
  end
end

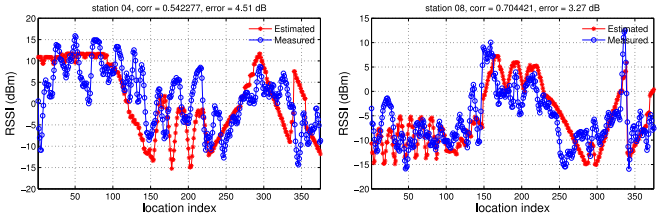

Fig. 9. Comparison between model-generated RSS estimation with actual measurements, for FM station 4 and 8, respectively. The cross-correlation is 0.54 and 0.70, and the median error is 4.5 and 3.3 dB, respectively.

4.2 Model Verification

In order to verify the model accuracy, we pick the third site and compare the actual measurements with the output values from our model. We take measurements from 375 actual spots within the thrid site and measure the RSSs at each of the spots. Fig. 9 shows the RSS estimations together with actual measurements at those spots. While the estimation does not perfectly match with the measurements, we can visually see the similarity in the trend between the two. For detailed verification of the model accuracy, please see Section 7.2.

5 System Description

5.1 Overview

ACMI runs in two separate modes. Fig. 10 depicts the overall architecture. During the offline phase ACMI builds the FM fingerprint DB using the proposed propagation model. This offline operation is one-time process which is performed autonomously without any participation from users. The output of this offline phase, fingerprint DB, is provided to mobile users who want to navigate through the building. As the innate discrepancy exists between the model and the actual RSS distribution, a mobile user can perform online adjustment phase in order to further improve the accuracy. The online phase comprises runtime parameter calibration and path matching.

5.2 Offline Phase

FM fingerprint database is built offline using our RSS estimation model. We utilize the information source described in Section 3.1 as the input. Since we have already explained the offline procedures in the previous section, we omit any further detail here.

5.3 Online Phase

ACMI performs DB look-up to find out the current indoor position. This look-up is based on simple minimum squared error matching. Current position L is estimated to be a location in DB of which the RSS vector has the smallest euclidean distance with the measurement. L is formally given as $\arg\min_s ||\overrightarrow{RSS_{DB}}(s) - \overrightarrow{RSS_M}||$ where $\overrightarrow{RSS_{DB}}(s)$ is the estimated RSS vector in DB at an indoor spot s and $\overrightarrow{RSS_M}$ is the measured RSS vector at the mobile user's current location.

At this point the room identification shows large deviation ranging between 59 and 89 percent. The main cause is the errors in the outdoor path loss estimation. This estimation is not always accurate because of weather or unknown

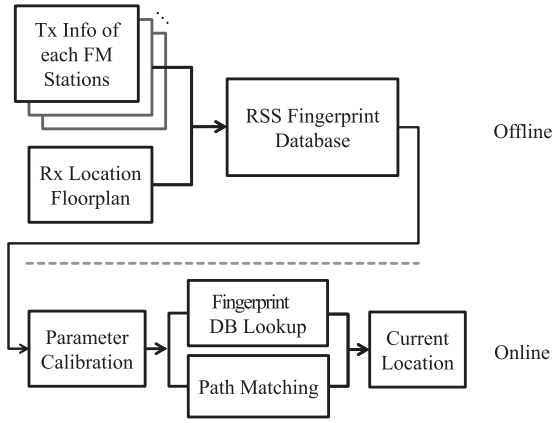

Fig. 10. Architecture of ACMI.

surrounding obstacles. Variability of antenna gains in mobile devices can also have some impact on this. The site-specific model parameters are another reason. The parameters are not uniform across buildings because of diversity in building materials. Therefore the runtime calibration is essential to correct these values.

But the calibration still does not guarantee the perfect capture of real RSS distribution. Ambiguity arises when multiple spots across the fingerprint DB exhibit similar RSS signatures. This causes localization error. One easiest remedy is to crosscheck as many signal sources as possible, e.g., 32 FM signals as in [9]. But such abundance might not be always available.

We perform path matching to improve the localization accuracy. The path matching *clusters* multiple indoor spots along the walking path of a mobile user. The basic motivation of path matching is that, even though the RSS estimation at each individual spot is not perfectly accurate, the *RSS changing pattern* over the broader area can be unique with much higher probability. For instance, imagine a scenario where a mobile user moves away from one of windows toward the inner part of a building. It is natural that the RSS gradually decreases with the distance to the window while slope of the curve might vary. The accuracy can be substantially improved by matching between a cluster of measured RSSs along the walking path and the estimated RSSs. The final result is 89 percent room identification and 6 m localization accuracy.

5.3.1 Runtime Calibration

The runtime calibration is a two-step process where the unknown parameters are derived first and then RSS DB is refined. $max(RSS(t))$, α, f and C_1 in Eq. (3) are the parameters to be calibrated. ACMI mainly performs the calibration at known reference points, e.g., a building entrance. The reference point is defined a priori and its exact location is readily known to the system.

The calibration process is triggered when a mobile user walks into the reference point. Starting from the reference point, RSSs are sampled at multiple spots as the mobile user takes steps. The sampled RSSs are compared with the estimated RSSs at the same locations to calibrate the parameters. Exact location of each step is indeed hard to know, but we rely on the walk detector that uses motion sensors in a

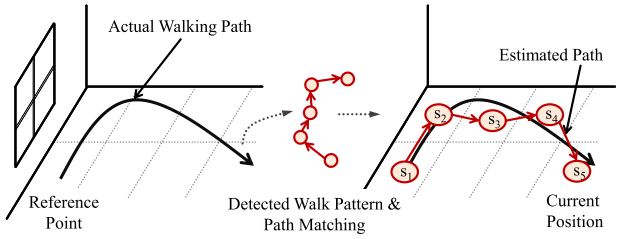

Fig. 11. Indoor positions along the walking path are recognized by walk detection. The detected positions are used to (1) calibrate the model parameters and to (2) perform the path matching.

smart device to infer the approximate location. We further describe this in Section 5.3.2. In our setup, we use five nearby spots for the calibration, as shown in Fig. 11.

At each spot the largest RSS component should be decided among RSS_{LoS}, RSS_{NLoS} and RSS_{ind} according to Eq. (1). Usually either LoS or NLoS signal component dominates at the building entrance. The stronger component of the two is decided based on the following simple rule; if a transmission tower is visible the LoS signal will dominate; otherwise the NLoS signal will. Only in case a certain reference point is isolated and does not have direct path to any source of signals, then the indirect component should be selected.

Once the strongest component has been determined the simple solution should be to directly solve the linear equations for the parameters since we have only a fixed number of unknowns. However, the RSS samples in real world always include measurement noises for various reasons, e.g., changes in the orientation of antennas or existence of surrounding objects. It is therefore required to choose optimal values that minimize the estimation errors.

LMS-based calibration. Assume that the NLoS signal is strongest at a certain reference point. Then Eq. (3) is re-written as

$$Y = H \cdot X + W,$$

where Y is l-rank measurement vector $[y_1 \cdots y_l]$ with y_i the measured RSS at location $i = 1 \cdots l$, H is the array of parameters $[max(RSS(t)), \alpha, f, C_1]$ to be calibrated, X is l-rank vector $[x_1, \ldots, x_l]$ such that each x_i is $[1, -10 \cdot log_{10}(d_i/d_0), -n_i, 1]^T$ and W is the measurement noise. Here H and X are defined to reformulate Eq. (3). The minimum mean squared error (MMSE) is known to provide optimal solution when the measurement noise exists. But it requires the knowledge of C_X, the auto-covariance matrix of X, that is not available in our case.

We use the least mean square filter. The LMS filter does not require the knowledge of C_X but is proven to converge to a solution equivalent to MMSE [32]. In LMS, the parameter vector H is updated as:

$$H_{i+1} = H_i + \mu \cdot e_i \cdot x_i,$$

where μ is a small constant and e_i is defined as $e_i = Y_i - H_i \cdot x_i$. RSS vector Y_i is measured at step i where each measurement step is notified by the walk detector. H_i is then iteratively updated to minimize the error term e_i. We expedite the computation by assigning the measured values from experiments as an initial seed for H_0. In our implementation, it took measurements at less than 5 locations to converge.

So far we only described the NLoS case but the same steps apply for RSS_{LoS} and RSS_{ind}. The elements in H and X are replaced with corresponding ones accordingly.

Refinement of fingerprint DB. With the calibrated parameters, the fingerprint DB should be re-generated and offered to the user. The user can simply report the parameters to the service provider, where the DB is automatically refined based on the parameters.

5.3.2 Path Matching

ACMI samples and keeps l-recent RSS measurement vectors in the buffer. While performing the localization, ACMI continuously checks for ambiguity. We define that estimation is *ambiguous* when the matching error at a spot s is large, formally given as:

$$||\overrightarrow{RSS_{DB}}(s) - \overrightarrow{RSS_M}|| > \theta_{amb}.$$

When the ambiguity is detected ACMI starts looking into the buffer to find a path $P = [s_0, \ldots, s_{l-1}]$ such that

$$P = \arg\min_{s_i \in S} \sum_{j=0}^{l-1} ||\overrightarrow{RSS_{DB}}(s_j) - \overrightarrow{RSS_M}(j)||,$$

where $\overrightarrow{RSS_M}(j)$ is the jth measured RSS vector in the buffer and l is the maximum buffer length. After the path is chosen, s_{l-1}, the last spot in the matched path, is finally estimated to be the current location.

Then the question is how to choose the candidate spots $\hat{s_0}, \ldots, \hat{s_{l-1}}$. Given that the total number of indoor spots is $|S|$, to find the best match among all the possible combinations will incur $|S|^l$ computations. To reduce the search space, we extract the user walking pattern. Each $\hat{s_{i+1}}$ is dead-reckoned from $\hat{s_i}$ based on the motion sensors in the smart device. We regulate the distance between two successive spots such that $||\hat{s_i} - \hat{s_{i+1}}|| = d_{const}$ to relate only neighboring spots with the pre-defined fixed interval. The two conditions are forced by the walk detector. The result is $O(|S|)$ number of candidate spots that meet the detected walking pattern.

Walk detector. Our walk detector reports the short term topology of a user's walk path. Accelerometers in smartphones can measure the acceleration in three dimensions. This information can be used to calculate the displacement of a mobile user. We take accelerometer readings and rotate the readings to make z-axis aligned with the direction of gravity using the compass readings as detailed in a study [33]. Fig. 12 shows raw three-axis accelerometer readings and their rotated readings with the gravity value extracted from z-axis readings. Fig. 12 also shows steps and heading directions extracted from the rotated readings that allow us to estimate short term displacement vectors. In our indoor experiments, we verified that steps can be perfectly detected when a proper threshold on acceleration is applied and heading directions can be estimated with errors less than 19 angular degree.

Note, however, that our system does not attempt to infer the user's location directly from the sensor readings

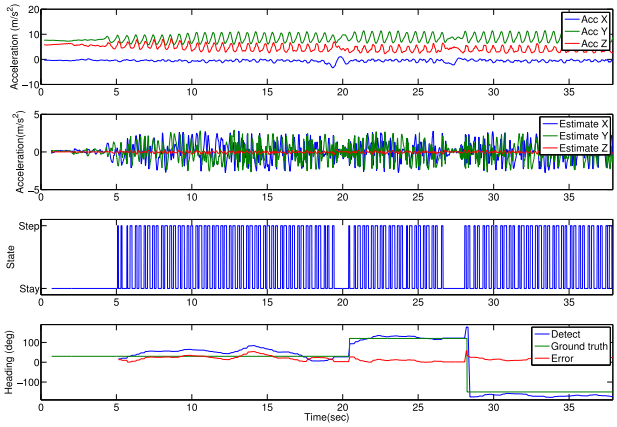

Fig. 12. (a) Accelerometer readings of three-axis in a random position, (b) accelerometer readings rotated to align with heading direction based on compass readings where gravity is subtracted from z-axis readings, (c) steps of a walk detected from the swing patterns in the rotated readings, (d) the heading directions with three directional changes estimated by the rotated readings.

and the resulted dead-reckoning technique. Rather, the primary role of our walk detector is to obtain the short term topology of mobile user's walk path. We only use the short term topology, so there is no need for the periodic calibration of sensors which is essential for dead-reckoning techniques since it can still provide the walk pattern with reasonable accuracy. This detected walk pattern is then used to reduce the search space in the path matching phase. We present the walk detector performance in Section 7.4.

6 Discussions

6.1 Possible Limitation

If a floorplan itself does not properly reveal the sufficient structural information it is difficult to estimate the indoor RSS. For instance, consider a building of which the ceiling itself is a large window. Our current approach cannot effectively deal with the case since we only utilize 2D information obtained from the floorplan. However, this is also not a fundamental challenge. We can extend our 2D floorplan-based model into 3D one once the whole set of information about the building is provided.

6.2 Signal Attenuation

Obstacles around the building might block the propagation and therefore weaken the FM signals. This situation may frequently happen in downtown areas. However it has been experimentally shown that the proportion of FM signal degradation is not significant [34], [35], [36]. The measurement study in San Francisco downtown area [36] shows that the signal impair was at most 7.3 percent in the worst case. This implies that the FM signals are obtainable indoors most of time. This is empirically true as most radio stations are audible in downtown areas. The signals might be much weaker in such areas, but recall that our system does not rely on the exact RSS value but the relative attenuation pattern within the building. The indoor attenuation pattern is invariant regardless of outdoor attenuation and we can still perform path matching to find specific RSS changing patterns to find the indoor position of a user.

We have already experienced similar situation in our experiment. When the height of a transmission tower is short (station 1 in Table 2) or a tower is located far away (station 2 and 6 in Table 2), the transmitted signals experience significant attenuation before reaching the surfaces of a building and therefore there exist very little difference in LoS and NLoS signals (Fig. 6). But we are still able to use the information to perform the indoor localization via the path matching.

6.3 Floor Differentiation

ACMI can naturally differentiate between the floors when each floor has distinctive indoor structures. This structural difference will create unique RSS distribution and each floor will appear like a completely different location. We can integrate them into a single RSS DB. A mobile user can search the current position from this multi-floor DB. A point in any floor, having the minimum RSS error with the RSS measures, will be chosen to be the current position.

What happens if the indoor structures are similar between floors? Still, if each floor has large enough difference in height (e.g., larger than 10 m), floors will exhibit different RSS distribution [31]. This is because signals traversing through different height would experience different path losses.

Inevitably ACMI might show limited ability if the floors have similar indoor structures and the height difference is not significant as well. In this case each floor will exhibit similar RSS distribution and therefore ACMI will struggle to find the correct user location among several candidate positions distributed across multiple floors. This makes the floor differentiation less practical if ACMI is to be used alone. Rather we can combine other techniques to find the floor. One possible solution might be to notify a mobile user of the current floor when the user gets to a certain floor. This can be implemented in various ways e.g., using an embedded barometer sensor or Bluetooth (or WiFi) signaling.

Please note that floor differentiation was not considered as a potential use case when we designed ACMI. In many cases we can safely assume that a user can find the current floor he is located in without much difficulty. This is because a user usually chooses a specific floor proactively when he decides to move between floors. At the point when a user changes floor, he can easily find signs that indicate the floor.

6.4 Reference Point Recognition

A mobile user can manually notify ACMI, of the current location, when she visits a reference point. Reference points can be chosen from frequently visited landmarks. But it may true that users cannot always accurately pin-point their positions.

ACMI can try to automatically recognize reference points. It is achieved by detecting the distinctive RSS characteristic at a spot. During the runtime ACMI keeps looking for an indoor spot s where any element of the measured RSS becomes the maximum, i.e., $RSS_M(s,t) = max(RSS(t))$ for any $t \in T$. This indicates that a mobile user is near one of LoS windows and greatly reduces the ambiguity in inferring the user's location. As the false positive detection will

TABLE 3
Locations in a Department Building (MRC) Where RSS Measurements Were Performed

Location (floor)	# of spots	Area (m^2)	# of rooms
MRC (second)	36	2,990	46
MRC (third)	86	2,990	55
MRC (fourth)	375	2,990	69
EB-E (first)	147	4,550	28
EB-E (second)	129	4,550	59
EB-E (third)	119	4,550	69
EB-W (first)	217	4,550	23

lead to ill calibration of parameters, we trigger the reference point detection when $|RSS_M(s,t) - max(RSS(t))|$ is small.

Alternatively, an assistive signal from bluetooth emitters installed at a few reference points can explicitly notify the mobile device when to calibrate. The measured signal at the position can be used to calibrate the model parameters, and to correct the estimation of the current location as well.

6.5 Complexity

We discuss how to further reduce the complexity of online path matching. If it is detected that a user has come back to the previously visited location there is no reason to continue the matching operations. In this case ACMI resets the path matching. ACMI continuously checks if the following condition is met whenever a new RSS is sampled:

$$||\overrightarrow{RSS_M} - \overrightarrow{RSS_M}(i)|| < \theta_{dup} \quad for\ i = 1 \cdots l,$$

where θ_{dup} is pre-defined threshold. When the condition is met, ACMI determines that the user came back to the previous location, empty the buffer and restart the path matching from the next step.

Another way to reduce the computation is to filter out the erroneous candidates earlier while performing the path matching. In path matching, ACMI traces back the buffered RSS samples to find the path $P = s_0, \ldots, s_{l-1}$ that shows the minimum RSS difference. If a segment of a certain path shows large RSS difference, there is no need to further look into remaining candidate spots along the path. For example, if $RSS_M(s_{l-1}) > \theta$, all the paths $P = \ldots, s_{l-1}$, ending at s_{l-1} can be immediately ignored.

7 Evaluation

In this section, we verify if our indoor signal propagation model accurately captures the actual RSS distribution. We then study the impact of receive antenna on RSS and walk detector accuracy in various configurations. Finally we examine the localization accuracy of the model combined with the proposed online processing.

7.1 Experiment Setup

We perform measurements and collect RSSs at 1,109 spots in seven different locations, shown in Table 3. These are the department buildings in campus of about 35 m × 85 m (MRC) and 55 m × 85 m (EB-E and EB-W) area in which each floor has different indoor structures. We use USRP1 with a laptop computer to collect the data. Signals from eight FM stations are used as described in Section 3.

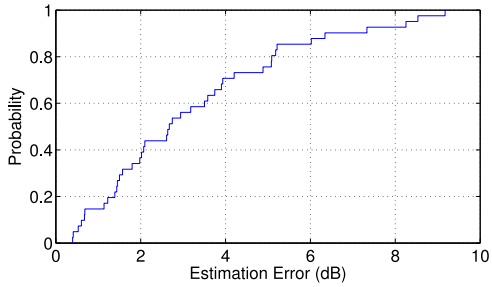

Fig. 13. CDF (cumulative density function) of signal estimation error in dB.

We also implement the walk detector on Android platform with Android 4.4.2. We verified that our walk detector works well on various Samsung, LG and Sony smartphones with Quad-core snapdragon processors from Qualcomm. Out of many smartphones, we used a widely sold Samsung Galaxy Note 2 to evaluate our walk detector performance. We use the path and distance information reported by the walk detector together with the RSS log to obtain the indoor position.

7.2 Modeling Accuracy

Fig. 13 shows the distribution of estimation error of signals from eight stations in all location. The calibration has been performed and so the outdoor path loss estimation error is not included. It is shown that our model achieves the 70th percentile error of 4 dB. Fig. 14 demonstrates the modeling accuracy more intuitively. It shows the euclidean distance between RSS vectors in two different locations, MRC fourth floor and EB-E second floor. The left figures of each set show the self-distance of RSS measurement vectors. The diagonal line is clearly shown in blue, which means that the euclidean distance is zero between same set of RSS vectors. The RSS measurement and estimation vectors (without calibration) are compared in the right figures. While the

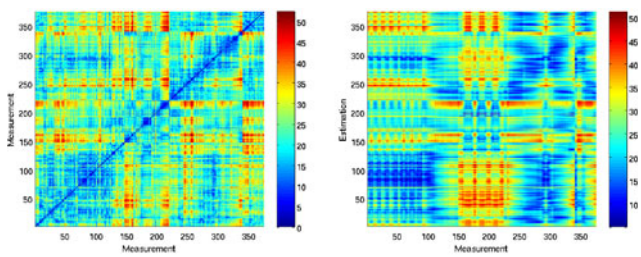

(a) Euclidean distance representation of RSS vectors in MRC 4th floor.

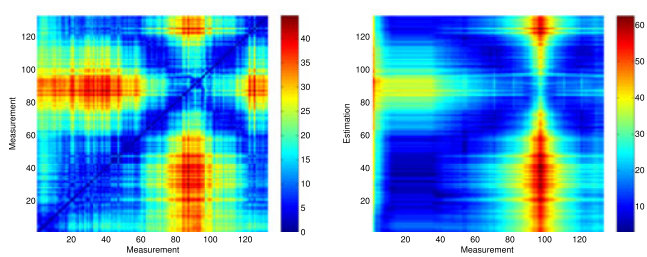

(b) Euclidean distance representation of RSS vectors in EB-E 2nd floor.

Fig. 14. Euclidean distance representation of RSS vectors where *X*- and *Y*-axis represent the indoor spot index. Left figures show the euclidean distance between measurement vectors and right figures show measured and estimated vectors. The area in blue shows more similarity between two vectors than red.

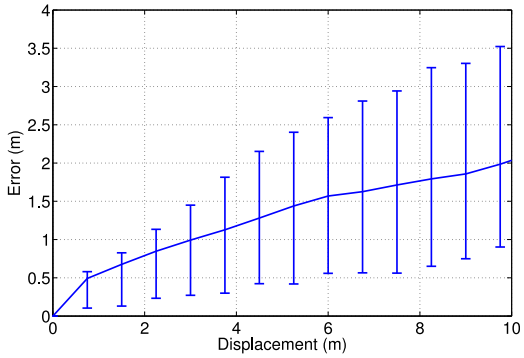

Fig. 15. The positioning error, estimated with mobile sensors, increases as a user takes steps. The graph shows 90 percent confidence intervals of positioning errors for 50 times' runs of 10 m walk.

diagonal line is not visible at a glance, we can still observe bluish area in both figures along the diagonal line. This means that even though not perfectly accurate as the real measurements, the model captures the way signals are propagated indoors. When MSE matching is applied to estimate indoor locations, we observe that the localization accuracy ranges from 10 to 18 m, which will be more clarified in Fig. 17.

According to our observation, there are three reasons lowering the accuracy of our model. The first reason is the internal structures of a building. If the internal structure does not create distinct RSS signatures, e.g., an open space without many obstacles, there is not much differentiation in RSSs between nearby spots. Then the localization accuracy will drop. The second reason is with the initial modeling parameters. We observe that the runtime calibration improves the accuracy around 6 meters at engineering buildings (EB-E-1,2,3 and EB-W-1). This is mainly because the initial parameters were measured in a different building (MRC fourth floor) and they are quite different at other locations. On the other hand, measurement results at MRC shows no significant improvement in accuracy after the calibration. The third reason is more fundamental. If there are structures that do not appear in the floorplan, the RSS distribution cannot be correctly modeled. Even with online calibration, there will still be some modeling errors. Per our observation, metal objects such as steel desks or shelves induce path loss almost comparable to indoor walls. This can be indeed mitigated using more signal sources. If there are signals from various directions, the unexpected obstruction that some signals experience will have less impact on the RSS vector.

7.3 Impact of Antenna

FM antenna is the crucial piece of our system. Here we study its impact on RSS values in various configuration. We use one of the most advanced smartphone as of now, Sony Xperia Z Ultra with LTE capability. The device gets FM signal through an earphone cable plugged in as an antenna. We measure the RSS in the following setups: 1) RSS when the antenna is plugged/not-plugged. When an earphone is plugged and tuned to a FM radio station that we can clearly hear stereo sound, the RSS goes beyond 50 dBm and in our area it was maxed out at 54 dBm. For other FM radio stations, the RSS ranges from 39 to 54 dBm. When tuned to a radio frequency with no FM radio station, the RSS goes flat down to 21 dBm. Unplugging the earphone gives the same flat RSS. 2) RSS when the antenna is fold/stretched. Folding or stretching the antenna makes almost no difference in the RSS. In few cases, the RSS varies by 1 dBm but mostly there is no change. 3) RSS when the antenna is in the pocket/hand-held/wore. Similarly to folding, putting the entire antenna in the pocket makes very minor difference. The RSS degrades only by 2 to 3 dBm. Holding or wearing the antenna also does not significantly change the RSS. It only changed the RSS by 2 to 3 dBm. 4) RSS with the various antenna direction. When the heading direction of the body changes, the RSS changes quite a lot. This may be from the signal blocking or capturing effect of human body. Our observations show that turning 360 degree at a single position made RSS difference ranging from 5 to 15 dBm.

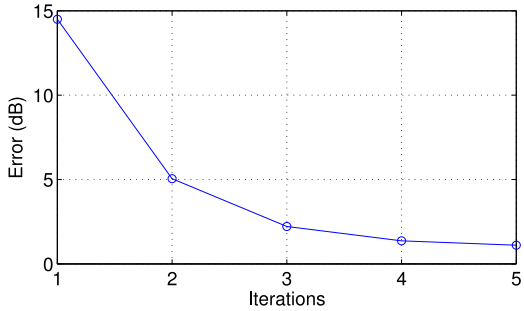

Fig. 16. Model parameters (outdoor RSS here) quickly converges to real values with the learning algorithm.

Our observations on the impact of antenna clarifies that ACMI's signal map matching would work fine no matter what the antenna holding position is unless there is no holding direction change during the localization process.

7.4 Walk Detector Accuracy

We detect the user movement using accelerometers and compass as explained previously. Fig. 15 shows the error performance of our walk detector as a user takes steps. Our tests with 50 runs show that the average error of about 2 m is resulted after a user moves 10 m. The 90 percent confidence intervals confirm that majority of 10 m tests have less than 3.5 m positioning error. Overall, the walk detector could extract a user's walking pattern with reasonable accuracy to use for the DB matching but the error monotonically increases as a user moves. Therefore, in order to limit the amount of errors, we only use the most recent 10 m estimation of our walk detector for the DB matching.

7.5 Calibration Process

There are innate discrepancies between model parameters with actual values. The online calibration adjusts errors in model parameters such that the modeling accuracy can be improved. Fig. 16 shows that one of the model parameters, outdoor RSS, converges to the actual value with LMS iteration. Even though the initial error was very large, around 15 dB, it shrinks to around 1 dB after five rounds of iterations.

7.6 Localization Performance

We test the localization performance of ACMI at different locations. Three cases, (1) simple DB look-up with no additional online processing (None), (2) online calibration and (3) online path matching after the calibration (Calib.+PM),

TABLE 4
The Number of Detected Reference Points and the Trained Parameters at Each Location

Location(floor)	Ref.	α	f (dB)	C (dB)
MRC (second)	1	2.15	6.2	7.7
MRC (third)	3	2.15	7.0	7.3
MRC (fourth)	8	2.16	6.3	7.5
EB-E (first)	3	2.58	6.4	6.9
EB-E (second)	2	2.56	6.9	6.5
EB-E (third)	3	2.56	6.2	6.5
EB-W (first)	3	2.63	5.4	6.1

are shown. For the online calibration we first notified ACMI of the initial location at the entrance of buildings. As we roam around within the buildings, ACMI automatically recognized additional reference points and performed further calibration and correction of the estimated locations. Since the false positive is more harmful we made it conservative such that ACMI detects the reference point only when it is very certain. The parameters are shown in Table 4.

Fig. 17 shows the evaluation results. Without any online operation, the localization accuracy entirely depends on the modeling accuracy and it varies from 10 to 18 meters. Online calibration reduces the error in places where the model parameters have significant difference with initial values. After the path matching the accuracy becomes around 6 meters. For the path matching, we used the maximum path length of 5. Fig. 18 shows the error distribution after the path patching. In all of dataset, the error is less than 10 m with 60 percent probability.

The room identification ranges between 59 and 89 percent between any online operation and improves up to 89 percent on average after the path matching. Note that the room identification accuracy does not align with the localization accuracy since it also depends on the size of rooms. For example, in MRC-4 there are many small private offices with sizes less than 12 m^2 so the accuracy is around only 60 percent.

7.6.1 Accuracy in Downtown Area

One of possible concerns with FM-based indoor localization is with its performance in downtown areas. The signals

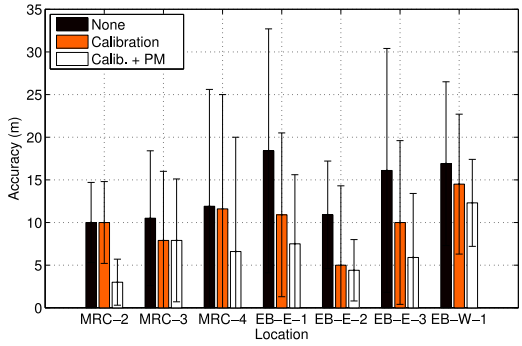

(a) Average localization accuracy with 95% confidence interval.

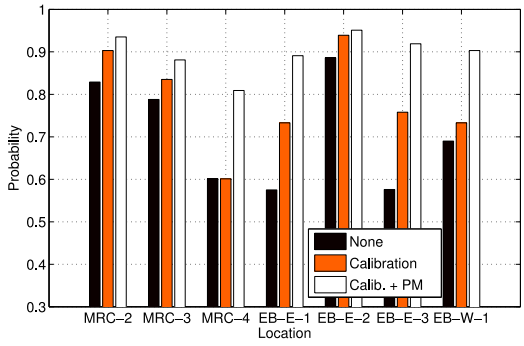

(b) Room level identification accuracy.

Fig. 17. Localization accuracy at different floors of several campus buildings.

transmitted from remote FM stations would be frequently blocked by buildings and therefore the RSS estimation might be highly inaccurate.

This was partly true when we conducted the evaluation in downtown area. We evaluated ACMI in three different buildings, two public museums and a shopping mall, where their floorplan is openly accessible. Fig. 19 shows the result. The initial localization, without any further processing, was poor with more than 20 m errors. This is because the RSS becomes much weaker at a local building in the downtown areas and there are frequent DB mismatches.

However the localization becomes a lot more accurate with online calibration process. The calibration brings about

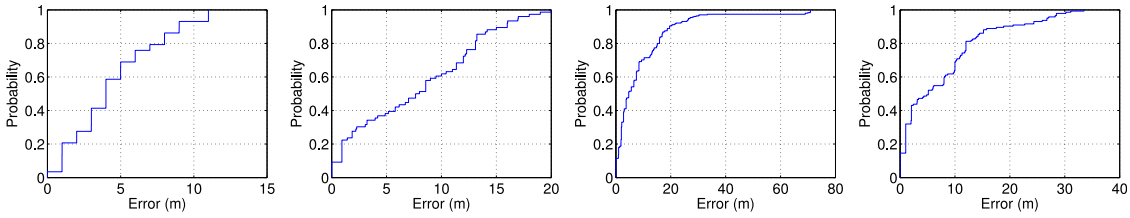

(a) MRC-2. (b) MRC-3. (c) MRC-4. (d) EB-E-1.

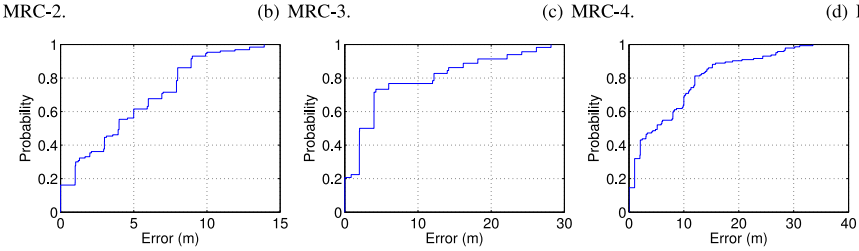

(e) EB-E-2. (f) EB-E-3. (g) EB-W-1.

Fig. 18. CDFs of localization errors in meters of ACMI at different buildings after performing path matching.

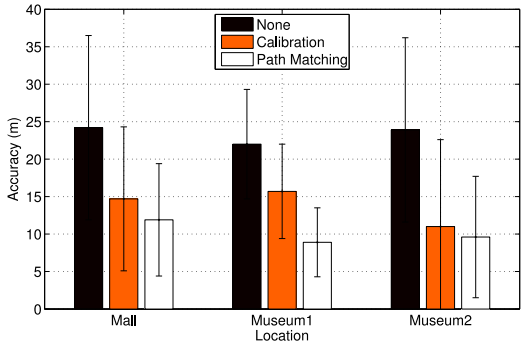

Fig. 19. Localization accuracy of ACMI in downtown areas.

40 percent improvement in the localization accuracy. During the calibration process ACMI quickly learns about the changed RSSs because the change is usually constant in indoor locations.

7.6.2 Scaling with Number of FM Stations

We use signals from only eight stations due to the limited availability in our area. As we would like to see the system performance when there are more FM stations, we perform simulations in the following way. In addition to the existing RSS traces we generate signals from virtual FM stations. The virtual FM stations are assigned the average values of transmission power and antenna height calculated from the real FM stations. Then they are distributed around the building with random distances and directions. To make it realistic, we manually add random measurement errors that amount to the modeling errors measured from our earlier experiments. We run the simulations 30 times for each number of stations. Fig. 20 shows the simulation results where up to 24 virtual FM stations are introduced. It is shown that with signals from 32 stations the localization accuracy improves up to 3 m without any online operations and below 1 m with runtime calibration and path matching.

7.6.3 RSS Dissimilarity between Signals from Different FM Stations

We survey the correlation of RSS distribution between signals from different FM stations using our measurement data. Fig. 21 shows the correlation coefficient with regard to the angle between stations. Even though it is not very significant, we can see that the correlation gradually decreases as the angle between two stations increases. If there are more FM stations scattered around the building we can expect that we can have more unique RSS distribution. On the other hand, if the FM stations are located in a similar direction from a building, the RSS distribution will be generally similar and the localization efficiency will become worse.

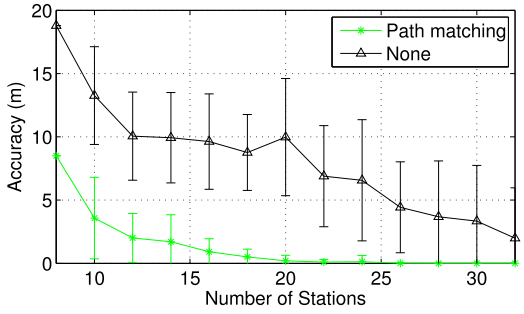

Fig. 20. Simulation results show that the performance of ACMI scales with number of FM stations.

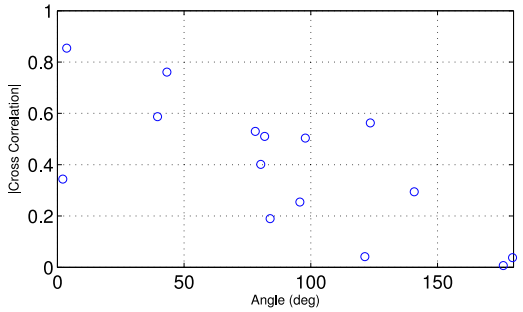

Fig. 21. The RSS distribution becomes more distinctive as the view-angle to the stations increases.

8 Conclusion

In this paper, we try to build an indoor localization system that does not require site survey. While there have been innovative proposals in the literature, we take a new approach that, by modeling the FM signal distribution over the floors, performs fingerprint-based indoor localization. While our empirical model is simple, we show that the model is effective and catches well RSS variations within a building with reasonably good accuracy. We further improve the accuracy using the online calibration and the path matching technique. In all of the processes, there is not much expenditure in time and cost for installation and running of this system. We believe that this proposal can suggest a new direction to the indoor localization research.

Acknowledgments

This work was supported in part by the US National Science Foundation grants (1016216, 0910868), the Ministry of Science, ICT & Future Planning (NRF-2014R1A1A1006330), and the Future Strategic Fund (1.140003.01) of UNIST. K. Lee is the corresponding author. A preliminary version of this paper was published in ACM Mobisys 2013.

References

[1] P. Bahl and V. Padmanabhan, "RADAR: An in-building RF-based user location and tracking system," in *Proc. IEEE INFOCOM*, 2000, pp. 775–784.

[2] M. Youssef and A. Agrawala, "The Horus WLAN location determination system," in *Proc. ACM 3rd Int. Conf. Mobile Syst., Appl. Services*, 2005, pp. 205–218.

[3] J. geun Park, D. Curtis, S. Teller, and J. Ledlie, "Implications of device diversity for organic localization," in *Proc. IEEE INFOCOM*, 2011, pp. 3182–3190.

[4] J.-G. Park, B. Charrow, D. Curtis, J. Battat, E. Minkov, J. Hicks, S. Teller, and J. Ledlie, "Growing an organic indoor location system," in *Proc. ACM 8th Int. Conf. Mobile Syst., Appl. Services*, 2010, pp. 271–284.

[5] A. Rai, K. K. Chintalapudi, V. N. Padmanabhan, and R. Sen, "Zee: Zero-effort crowdsourcing for indoor localization," in *Proc. ACM 18th Annu. Int. Conf. Mobile Comput. Netw.*, 2012, pp. 293–304.

[6] H. Wang, S. Sen, A. Elgohary, M. Farid, M. Youssef, and R. R. Choudhury, "No need to war-drive: Unsupervised indoor localization," in *Proc. ACM 10th Int. Conf. Mobile Syst., Appl. Services*, 2012, pp. 1977–210.

[7] Z. Yang, C. Wu, and Y. Liu, "Locating in fingerprint space: Wireless indoor localization with little human intervention," in *Proc. ACM 18th Annu. Int. Conf. Mobile Comput. Netw.*, 2012, pp. 269–280.

[8] Z. Zhang, X. Zhou, W. Zhang, Y. Zhang, G. Wang, B. Y. Zhao, and H. Zheng, "I am the antenna: Accurate outdoor AP location using smartphones," in *Proc. ACM 17th Annu. Int. Conf. Mobile Comput. Netw.*, 2011, pp. 109–120.
[9] Y. Chen, D. Lymberopoulos, J. Liu, and B. Priyantha, "FM-based indoor localization," in *Proc. ACM 10th Int. Conf. Mobile Syst., Appl. Services*, 2012, pp. 169–182.
[10] K. Chintalapudi, A. P. Iyer, and V. N. Padmanabhan, "Indoor localization without the pain," in *Proc. ACM 16th Annu. Int. Conf. Mobile Comput. Netw.*, 2010, pp. 173–184.
[11] Y. Ji, S. Biaz, S. Pandey, and P. Agrawal, "ARIADNE: A dynamic indoor signal map construction and localization system," in *Proc. ACM 4th Int. Conf. Mobile Syst., Appl. Services*, 2006, pp. 151–164.
[12] H. Lim, L.-C. Kung, J. C. Hou, and H. Luo, "Zero-configuration, robust indoor localization: Theory and experimentation," in *Proc. IEEE INFOCOM*, 2006, pp. 1–12.
[13] Federal Communications Commission, FM Database [Online]. Available: https://www.fcc.gov/encyclopedia/fm-query-broadcast-station-search, 2015.
[14] S. Sen, B. Radunovic, R. R. Choudhury, and T. Minka, "You are facing the Mona Lisa: Spot localization using PHY layer information," in *Proc. ACM 10th Int. Conf. Mobile Syst., Appl. Services*, 2012, pp. 183–196.
[15] J. Werb and C. Lanzl, "Designing a positioning system for finding things and people indoors," *IEEE Spectr.*, vol. 35, no. 9, pp. 71–78, Sep. 1998.
[16] X. Cheng, A. Thaeler, G. Xue, and D. Chen, "TPS: A time-based positioning scheme for outdoor wireless sensor networks," in *Proc. IEEE INFOCOM*, 2004, pp. 2685–2696.
[17] J. Xiong and K. Jamieson, "SecureAngle: Improving wireless security using angle-of-arrival information," in *Proc. 9th ACM SIGCOMM Workshop Hot Topics Netw.*, 2010, pp. 11:1–11:6.
[18] J. Krumm, G. Cermak, and E. Horvitz, "RightSPOT: A novel sense of location for a smart personal object," in *Proc. 5th Int. Conf. Ubiquitous Comput.*, 2003, pp. 36–43.
[19] P. Howland, D. Maksimiuk, and G. Reitsma, "FM radio based bistatic radar," *IEE Proc. Radar, Sonar Navigat.*, vol. 152, no. 3, pp. 107–115, Jun. 2005.
[20] P. Howland, D. Maksimiuk, and G. Reitsma, "FM radio based bistatic radar," *IEE Proc. - Radar, Sonar Navigat.*, vol. 152, no. 3, pp. 107–115, Jun. 2005.
[21] A. D. Lanterman, "Tracking and recognition of airborne targets via commercial television and fm radio signals," in *Proc. SPIE Acquisition, Tracking, Pointing XIII*, 1999, vol. 3692, pp. 189–198.
[22] A. Youssef, J. Krumm, E. Miller, G. Cermak, and E. Horvitz, "Computing location from ambient FM radio signals [commercial radio station signals]," in *Proc. IEEE Wireless Commun. Netw. Conf.*, 2005, pp. 824–829.
[23] D. C. Kelly, D. T. Rackley, and V. P. Berglund, "Navigation and positioning system and method using uncoordinated beacon signals," U.S. Patent 5 173 710 A, 1994.
[24] A. Matic, A. Papliatseyeu, V. Osmani, and O. Mayora-Ibarra, "Tuning to your position: FM radio based indoor localization with spontaneous recalibration," in *Proc. IEEE Int. Conf. Pervasive Comput. Commun.*, 2010, pp. 153–161.
[25] K.-W. Cheung, J.-M. Sau, and R. Murch, "A new empirical model for indoor propagation prediction," *IEEE Trans. Veh. Technol.*, vol. 47, no. 3, pp. 996–1001, Aug. 1998.
[26] G. Durgin, T. Rappaport, and H. Xu, "Measurements and models for radio path loss and penetration loss in and around homes and trees at 5.85 GHz," *IEEE Trans. Commun.*, vol. 46, no. 11, pp. 1484–1496, Nov. 1998.
[27] S. Seidel and T. Rappaport, "914 MHz path loss prediction models for indoor wireless communications in multifloored buildings," *IEEE Trans. Antennas Propag.*, vol. 40, no. 2, pp. 207–217, Feb. 1992.
[28] Z. Ji, B.-H. Li, H.-X. Wang, H.-Y. Chen, and T. Sarkar, "Efficient ray-tracing methods for propagation prediction for indoor wireless communications," *IEEE Antennas Propag. Mag.*, vol. 43, no. 2, pp. 41–49, Apr. 2001.
[29] R. Valenzuela, "A ray tracing approach to predicting indoor wireless transmission," in *Proc. IEEE 43rd Veh. Technol. Conf.*, 1993, pp. 214–218.
[30] C.-F. Yang, B.-C. Wu, and C.-J. Ko, "A ray-tracing method for modeling indoor wave propagation and penetration," *IEEE Trans. Antennas Propag.*, vol. 46, no. 6, pp. 907–919, Jun. 1998.
[31] C. Perez-Vega and J. Zamanillo, "Path-loss model for broadcasting applications and outdoor communication systems in the VHF and UHF bands," *IEEE Trans. Broadcast.*, vol. 48, no. 2, pp. 91–96, Jun. 2002.
[32] S. Haykin, *Adaptive Filter Theory* 4th ed. Englewood Cliffs, NJ, USA: Prentice-Hall, 2001.
[33] N. Roy, H. Wang, and R. Roy Choudhury, "I am a smartphone and i can tell my user's walking direction," in *Proc. ACM 12th Annu. Int. Conf. Mobile Syst., Appl. Services*, 2014, pp. 329–342.
[34] C.-E. Sundberg, "Digital audio broadcasting in the fm band," in *Proc. IEEE Int. Symp. Indust. Electron.*, 1997, vol. 1, pp. SS37–SS41.
[35] I. Smith, J. Tabert, T. Wild, A. Lamarca, Y. Chawathe, S. Consolvo, J. Hightower, J. Scott, T. Sohn, J. Howard, J. Hughes, F. Potter, P. Powledge, G. Borriello, and B. Schilit, "Place lab: Device positioning using radio beacons in the wild," in *Proc. 3rd Int. Conf. Pervasive Comput.*, 2005, pp. 116–133.
[36] "Report of the field test task group; field test data presentation," National Radio Systems Committee, Tech. Rep. NRSC-R52, 1996.

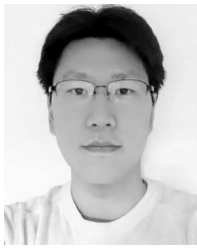

Sungro Yoon received the BS and MS degrees in computer science and engineering from Seoul National University in 2006 and 2008, respectively. He received the PhD degree in computer science from North Carolina State University in 2013. He is currently working on local search relevance under Bing group at Microsoft. His research interests include wireless signal processing, network protocol design, and indoor localization.

Kyunghan Lee (S'07-M'10) received the BS, MS, and PhD degrees in electrical engineering from Korea Advanced Institute of Science and Technology (KAIST), Daejeon, Korea, in 2002, 2004, and 2009, respectively. He is currently an assistant professor in the School of Electrical and Computer Engineering, Ulsan National Institute of Science and Technology (UNIST), Ulsan, South Korea. Prior to joining UNIST, he was with the Department of Computer Science, North Carolina State University, Raleigh, as a senior research scholar. His research interests include low latency networking, human mobility modeling, disruption tolerant networking, and context-aware mobile system design. He is a member of the IEEE.

YeoCheon Yun received the BS degree in electrical computer engineering from Ulsan National Institute of Science and Technology (UNIST) in 2013, where he is currently working toward the MS degree. His research interests include energy efficient mobile system design and cloud-powered network system design.

Injong Rhee (S'89-M'94) received the PhD degree from the University of North Carolina at Chapel Hill. He is a professor in the Department of Computer Science, North Carolina State University. He is an editor of the *IEEE Transactions on Mobile Computing*. His areas of research interests include computer networks, congestion control, wireless ad hoc networks, and sensor networks. He is a member of the IEEE.